A novel high performance TFS SJ IGBT with a buried oxide layer*

Zhang Jin-Ping(张金平)†, Li Ze-Hong(李泽宏), Zhang Bo(张 波), and Li Zhao-Ji(李肇基)

State Key Laboratory of Electronic Thin Films and Integrated Devices, University of Electronic Science and Technology of China, Chengdu 610054, *China*

(Received 2 January 2014; revised manuscript received 19 February 2014; published online 10 June 2014)

A novel high performance trench field stop (TFS) superjunction (SJ) insulated gate bipolar transistor (IGBT) with a buried oxide (BO) layer is proposed in this paper. The BO layer inserted between the P-base and the SJ drift region acts as a barrier layer for the hole-carrier in the drift region. Therefore, conduction modulation in the emitter side of the SJ drift region is enhanced significantly and the carrier distribution in the drift region is optimized for the proposed structure. As a result, compared with the conventional TFS SJ IGBT (Conv-SJ), the proposed BO-SJ IGBT structure possesses a drastically reduced on-state voltage drop ($V_{ce(on)}$) and an improved tradeoff between $V_{ce(on)}$ and turn-off loss (E_{off}), with no breakdown voltage (BV) degraded. The results show that with the spacing between the gate and the BO layer $W_o = 0.2$ μm, the thickness of the BO layer $L_o = 0.2$ μm, the thickness of the drift region $L_d = 90$ μm, the half width and doping concentration of the N- and P-pillars $W_n = W_p = 2.5$ μm and $N_n = N_p = 3 \times 10^{15}$ cm^{-3}, the $V_{ce(on)}$ and E_{off} of the proposed structure are 1.08 V and 2.81 mJ/cm^2 with the collector doping concentration $N_c = 1 \times 10^{18}$ cm^{-3} and 1.12 V and 1.73 mJ/cm^2 with $N_c = 5 \times 10^{17}$ cm^{-3}, respectively. However, with the same device parameters, the $V_{ce(on)}$ and E_{off} for the Conv-SJ are 1.81 V and 2.88 mJ/cm^2 with $N_c = 1 \times 10^{18}$ cm^{-3} and 1.98 V and 2.82 mJ/cm^2 with $N_c = 5 \times 10^{17}$ cm^{-3}, respectively. Meanwhile, the BV of the proposed structure and Conv-SJ are 1414 V and 1413 V, respectively.

Keywords: insulated gate bipolar transistor, trench field stop, superjunction, buried oxide layer

PACS: 85.30.–z, 85.30.De, 85.30.Pq, 85.30.Tv **DOI:** 10.1088/1674-1056/23/8/088504

1. Introduction

Owing to the superior performance derived from MOS gate control and bipolar conduction, insulated gate bipolar transistors (IGBTs) are widely used in a variety of power switching related areas, such as motor drivers, electric vehicles, power supplies, etc.[1–3] Over the last few years, IGBT performance has significantly improved due to the advent of trench gate, field stop (FS, also referred to as soft/light punch through) and carrier enhancement (such as IEGT, carrier stored, floating p layer, etc.) technology.[4–10] It has already becomes one of the mainstream power devices in medium-high voltage applications and its usage is continuously expanded due to the improvements in device performance. However, even for the advanced IGBT structure with all these three innovations, a certain thickness of the high resistive drift region is still required to sustain a certain breakdown voltage (BV), which sets a limit to further improvements in device performance.

The superjunction (SJ) concept featuring N- and P-pillars in the drift region was initially proposed to improve the tradeoff between the specific on-state resistance ($R_{on(sp)}$) and BV for high voltage unipolar devices, such as power MOSFET, etc.[11,12] The multiple junctions between pillars facilitate the depletion of the entire drift region at a lower voltage than a standard one-dimensional junction. Upon depletion, the pillars appear to be an intrinsic layer due to charge compensation. Therefore, a near uniform electric field distribution in the drift region is obtained with even higher doping concentrations of N- and P-pillars (N_n and N_p, respectively) and at the same time, a maximum of BV per unit length of the drift region is achieved. In recent years, commercial power MOSFET employing the concept were widely available owing to the fabrication process improvement for the SJ structure, which breaks the so-called 'limit of silicon' and enables the realization of devices with drastically reduced on-resistance.[13–15] Like MOSFET, the introduction of the SJ concept into IGBT not only significantly reduces the drift region thickness to withstand the same BV but also expedites the turn-off process due to the quick sweep of excess carriers by the fast expansion of the depletion region in N- and P-pillars.[16–19] Hence, as an advanced IGBT structure, the trench field stop (TFS) SJ IGBT demonstrates excellent overall performance. Compared with the conventional TFS IGBT without SJ structure, the TFS SJ IGBT possesses a reduced on-state voltage drop ($V_{ce(on)}$) and an improved tradeoff between $V_{ce(on)}$ and turn-off loss (E_{off}). However, unlike the SJ MOSFET, the SJ IGBT is a bipolar device with both N- and P-pillars conducting current during the on-state, owing to the conduction modulation effect. The $V_{ce(on)}$ and E_{off} are not only determined by the doping concentrations of the pillars N_n and N_p but also affected by the concentration of the excess carriers injected into the drift re-

*Project supported by the National Science and Technology Major Project, China (Grant No. 2011ZX02504-003), the Fundamental Research Funds for the Central Universities (Grant No. ZYGX2011J024), and the Open Foundation of State Key Laboratory of Electronic Thin Films and Integrated Devices, China (Grant No. KFJJ201301).

†Corresponding author. E-mail: jinpingzhang@uestc.edu.cn

© 2014 Chinese Physical Society and IOP Publishing Ltd

gion during the on-state. Therefore, in order to obtain further improved device performance to better meet the increasing demand in energy efficiency of power switches, it is important for the SJ IGBT structure to have an optimized carrier distribution in the SJ drift region during the on-state.

In this paper, for the first time, a novel TFS SJ IGBT with a buried oxide (BO) layer, which has an optimized carrier distribution in the SJ drift region, is proposed to further improve device performance. In the following sections, the proposed TFS SJ IGBT with BO layer and conventional TFS SJ IGBT structure are referred to as BO-SJ IGBT and Conv-SJ IGBT, respectively, unless otherwise stated.

2. Device structure and operation

Figure 1 shows the schematic cross sections of the TFS SJ IGBT structures: (a) proposed BO-SJ IGBT and (b) Conv-SJ IGBT. For the Conv-SJ IGBT structure, the reverse biased PN junction between N-pillar and P_{base} as well as the connection of P-pillar to P_{base} can extract the excess hole carriers in the drift region quickly in the turn-off process. However, during the on-state, this effect of the hole carrier extraction causes weak conduction modulation in the emitter side of the SJ drift region, especially when N_{n} and N_{p} are higher. This makes the carrier distribution in the SJ drift region unoptimized during the on-state and induce a large $V_{\text{ce(on)}}$ and unoptimized $V_{\text{ce(on)}}$ and E_{off} tradeoff. Compared with the Conv-SJ IGBT, the BO-SJ IGBT structure has an additional thin BO layer that is inserted between the P_{base} layer and SJ pillars inside the cell. Separating the P_{base} layer from the P-pillar and partial N-pillar, the BO layer acts as a barrier layer for the hole carrier in the drift region for the proposed structure. Therefore, the hole-carrier extraction from the SJ drift region is reduced, and the enhanced conduction modulation in the emitter side of the SJ drift region can be obtained. Hence, the carrier distribution in the drift region is optimized. The proposed BO-SJ IGBT device can be realized by using the conventional SJ process combined with partial silicon-on-insulator (SOI) technology or epitaxial growth technology from silicon with partial silicon-dioxide.[8,14,15,20,21] In the following sections, L_{d}, L_{b}, L_{c}, and L_{o} are the thicknesses of the drift region, N buffer, P collector, and BO layer, respectively. The W_{g}, W_{n}, and W_{p} denote half the widths of the gate, N- and P-pillars, respectively. W_{o} is the spacing between the gate and BO layer. The N_{b}, N_{c}, N_{n}, and N_{p} are the doping concentrations of the N buffer, P collector, N- and P-pillars, respectively. In order to make the discussion easier, the SJ structure discussed in the paper is a symmetric structure with $W_{\text{n}} = W_{\text{p}} = 1/2W$ and $N_{\text{n}} = N_{\text{p}} = N_{\text{d}}$. To have a meaningful comparison, the Conv-SJ with the same device parameters is also simulated. In the simulation, the lifetimes of electron and hole are both set to be 1 μs.

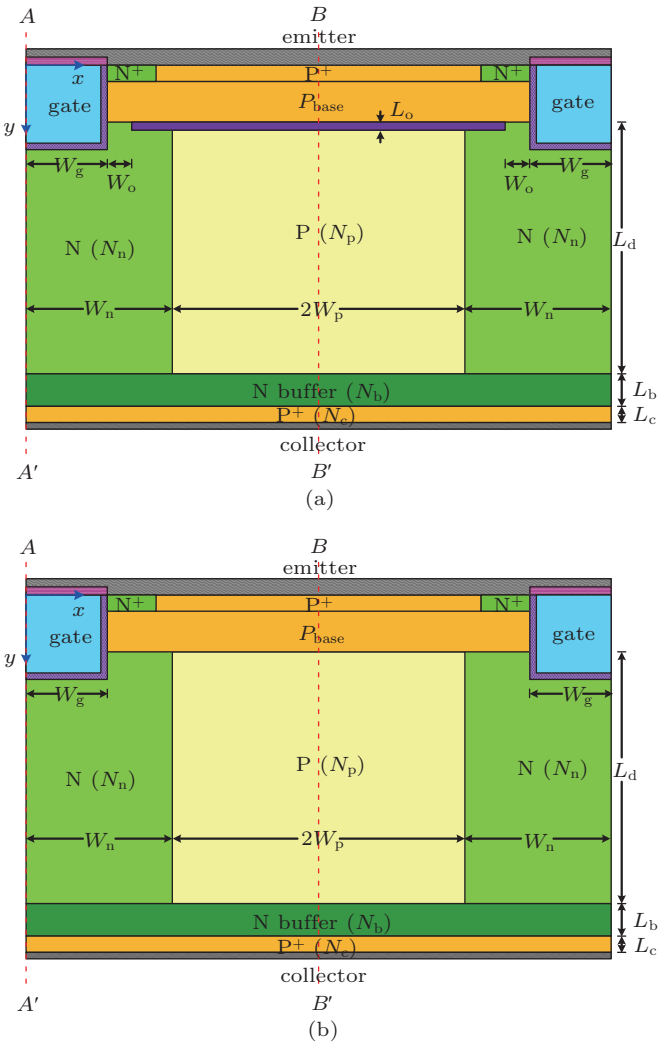


Fig. 1. (color online) Schematic cross sections of the TFS SJ IGBT structures: (a) proposed BO-SJ IGBT and (b) Conv-SJ IGBT.

3. Results and discussion

Figure 2 shows the influences of N_{d} on the $V_{\text{ce(on)}}$ for the two structures at $V_{\text{ge}} = 15$ V and $J_{\text{ce}} = 100$ A/cm^2. The parameters used in the simulation are $L_{\text{d}} = 90$ μm, $L_{\text{b}} = 4$ μm, $L_{\text{c}} = 1$ μm, $L_{\text{o}} = 0.2$ μm, $W_{\text{g}} = 1.5$ μm, $W_{\text{o}} = 0.2$ μm, $W = 5$ μm, $N_{\text{b}} = 2 \times 10^{16}$ cm^{-3}, and $N_{\text{c}} = 1 \times 10^{18}$ cm^{-3}. It can be seen from Fig. 2 that with N_{d} increasing from 1×10^{14} cm^{-3} to 1×10^{16} cm^{-3}, the $V_{\text{ce(on)}}$ of the proposed BO-SJ IGBT structure decreases from 1.09 V to 1.06 V. The higher the N_{d}, the lower the $V_{\text{ce(on)}}$ can be obtained for the proposed structure. However, for the Conv-SJ structure, $V_{\text{ce(on)}}$ is not a monotonic function of the N_{d}. The $V_{\text{ce(on)}}$ increases from 1.26 V (corresponding $N_{\text{d}} = 1 \times 10^{14}$ cm^{-3}) to a maximum of 2.05 V (corresponding to $N_{\text{d}} = 1.5 \times 10^{15}$ cm^{-3}) and when the $V_{\text{ce(on)}}$ reaches the maximum, it decreases to 1.23 V (corresponding to $N_{\text{d}} = 1 \times 10^{16}$ cm^{-3}). The $V_{\text{ce(on)}}$ of the proposed BO-SJ IGBT structure is much less than that of the Conv-SJ structure in a large range of the doping concentration of N- and P-pillars.

In order to have a better understanding of the effect of N_{d}

on $V_{ce(on)}$, the carrier distributions along AA' and BB' lines for the proposed BO-SJ IGBT structure are analyzed in Figs. 3(a)–3(d). The device parameters used in the simulation are the same as those in Fig. 2 with three fixed values of N_d. For comparison, the results of the Conv-SJ structure with the same device parameters are also shown in Figs. 3(a)–3(d). The simulated results in Figs. 3(a) and 3(b) show that for the Conv-SJ structure the concentrations of the minority carriers, hole–carriers along AA' line and electron–carriers along BB' line in the emitter side of the drift region are much lower than those in the collector side. Moreover, as N_d increases, the concentration of the minority carriers near the emitter side decreases drastically and the drift region with conduction modulation is reduced significantly. For the proposed BO-SJ IGBT structure, however, the whole SJ drift region is well conduction-modulated for these three values of N_d and the concentration of the minority carriers in the emitter side of the drift region is much higher than that for the Conv-SJ structure. The results in Figs. 3(c) and 3(d) show the distributions of the concentrations of the majority carriers, electron carriers along AA' line and hole carrier along BB' line. Due to the requirement of charge neutral in the drift region, the concentration of the majority carriers is a superposition of the concentration of the minority carriers and the doping concentration of the pillars N_d. Therefore, it can be seen that for the Conv-SJ structure the concentration of the majority carriers does not decrease monotonically with the increase of N_d, owing to the reverse effect of N_d and the conduction modulation effect. The contributions of both the majority and minority carriers to the current make the performance of $V_{ce(on)}$ for the Conv-SJ structure possess the result shown in Fig. 2. However, for the proposed BO-SJ IGBT structure, due to the strong conduction modulation in the emitter side of the drift region for various values of N_d, the concentration of the majority carriers increases as N_d increases and is much higher than that for the Conv-SJ structure. Therefore, it can be concluded that the smaller $V_{ce(on)}$ obtained for the proposed structure with different values of N_d is attributed to the optimized carrier distributions of the majority carriers and the minority carriers in the SJ drift region.

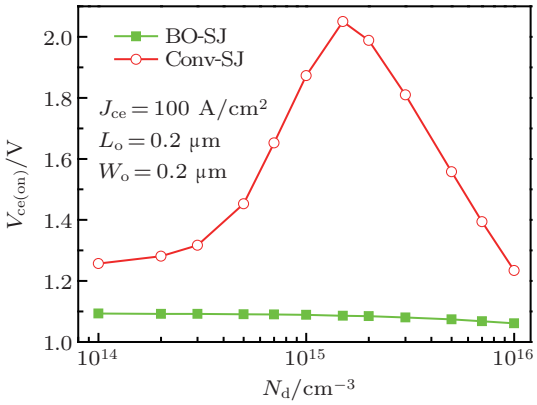


Fig. 2. (color online) Influences of N_d on $V_{ce(on)}$.

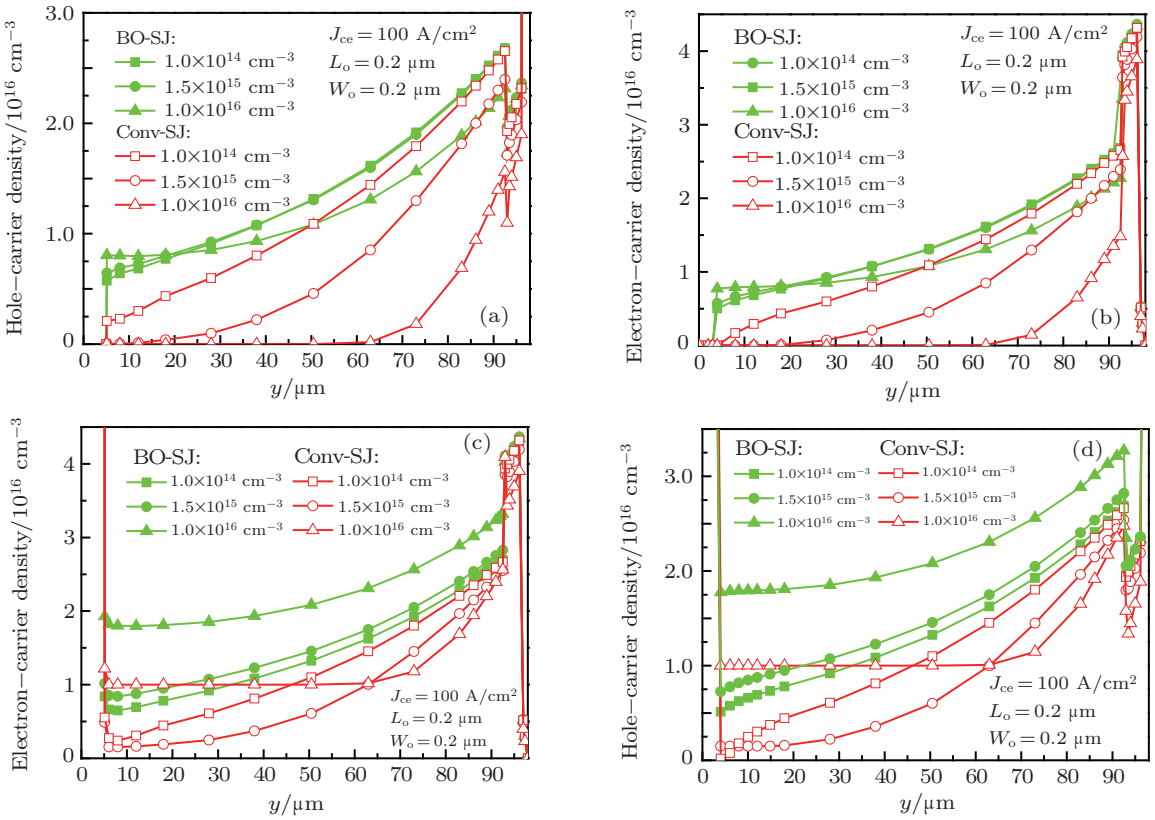


Fig. 3. (color online) Carrier distributions along AA' and BB' lines: (a) hole carrier along AA' line, (b) electron carrier along BB' line, (c) electron carrier along AA' line, and (d) hole carrier along BB' line.

Figure 4 shows a comparison of the simulated tradeoff curve between $V_{ce(on)}$ and E_{off} for the two devices with a clamped inductive load. The curves are obtained through the control of the collector doping concentration N_c. It can be seen that the tradeoff performance between $V_{ce(on)}$ and E_{off} for the proposed BO-SJ IGBT structure is much better than that for the Conv-SJ IGBT structure in a wide range of N_d. In addition, like the result in Fig. 2, it is found that better tradeoff performance can be obtained only for the Conv-SJ IGBT structure with a smaller or bigger value of N_d. However, for the proposed BO-SJ IGBT the tradeoff performance is improved with the increase of N_d and achieves nearly a saturation value when $N_d = 3 \times 10^{15}$ cm^{-3}. With $N_d = 3 \times 10^{15}$ cm^{-3}, the $V_{ce(on)}$ and E_{off} of the proposed structure are 1.08 V and 2.81 mJ/cm^2 with $N_c = 1 \times 10^{18}$ cm^{-3} and 1.12 V and 1.73 mJ/cm^2 with $N_c = 5 \times 10^{17}$ cm^{-3}, respectively. However, with the same device parameters, the $V_{ce(on)}$ and E_{off} for the Conv-SJ are 1.81 V and 2.88 mJ/cm^2 with $N_c = 1 \times 10^{18}$ cm^{-3} and 1.98 V and 2.82 mJ/cm^2 with $N_c = 5 \times 10^{17}$ cm^{-3}, respectively. Combining the results obtained above, it can be concluded that the improved tradeoff between $V_{ce(on)}$ and E_{off} for the proposed device is ascribed to the optimized carrier distribution in the SJ drift region.

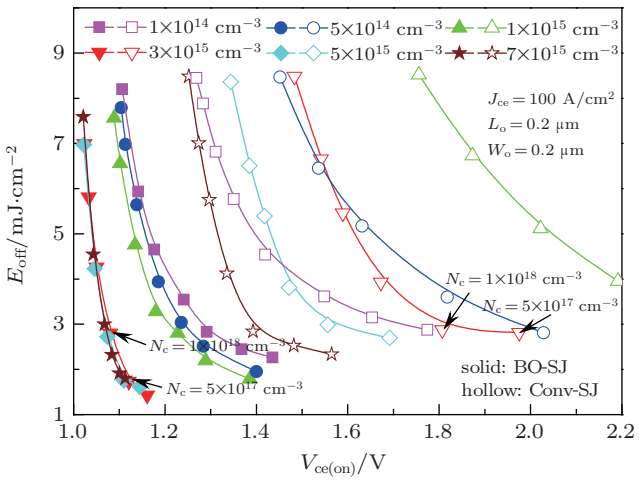


Fig. 4. (color online) Tradeoff curves between $V_{ce(on)}$ and E_{off}.

Figure 5 shows the influences of the N_d on the BV for the BO-SJ IGBT and Conv-SJ structures. It can be seen that the two structures have almost the same BV and the introduction of the BO layer has no negative influence on the BV. It can also be seen that for the two devices when the N_d is less than 3×10^{15} cm^{-3}, the BV keeps almost no change and when the N_d increases further, the BV starts to drop. The values of BV of the proposed structure and Conv-SJ with $N_d = 3 \times 10^{15}$ cm^{-3} are 1414 V and 1413 V, respectively. The inset in Fig. 5 shows the electric field distribution along BB' line and vertical line near the trench gate for the two structures with $N_d = 3 \times 10^{15}$ cm^{-3}. It can be seen that the electric field distribution is almost the same for the two devices except for a little difference at the BO layer. The two structures are broken down near the trench gate corner. The influence of charge imbalance ratio on BV for the BO-SJ IGBT is shown in Fig. 6. Since the Conv-SJ IGBT structure has almost the same result as the BO-SJ IGBT structure, the result of Conv-SJ IGBT is not shown in the figure. It is found that as the charge imbalance ratio increases, the BV of the SJ IGBT decreases. With the same charge imbalance ratio, the higher the N_d, the lower the BV obtained. Considering 5% of the charge imbalance ratio from the fabrication process, in order to meet the BV requirement of 1200 V, the N_d should not be larger than 3×10^{15} cm^{-3}. Therefore, considering the BV and the tradeoff between E_{off} and $V_{ce(on)}$, a good performance can be obtained for the proposed structure with $N_d = 3 \times 10^{15}$ cm^{-3}. In the following discussion on the design parameters of the BO layer, $N_d = 3 \times 10^{15}$ cm^{-3} will be used for the proposed device.

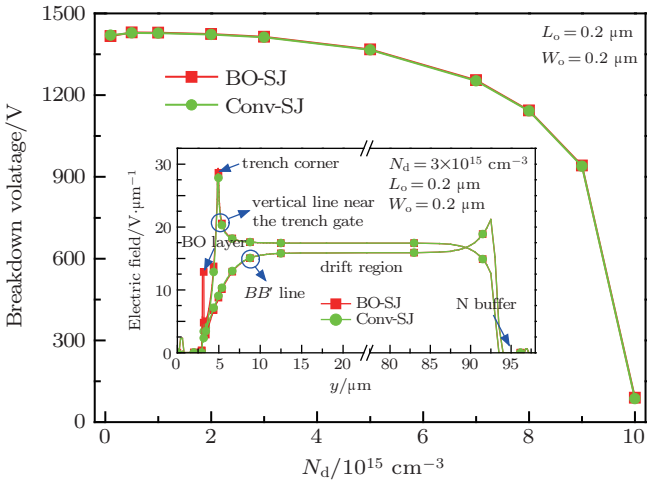


Fig. 5. (color online) Influences of N_d on BV.

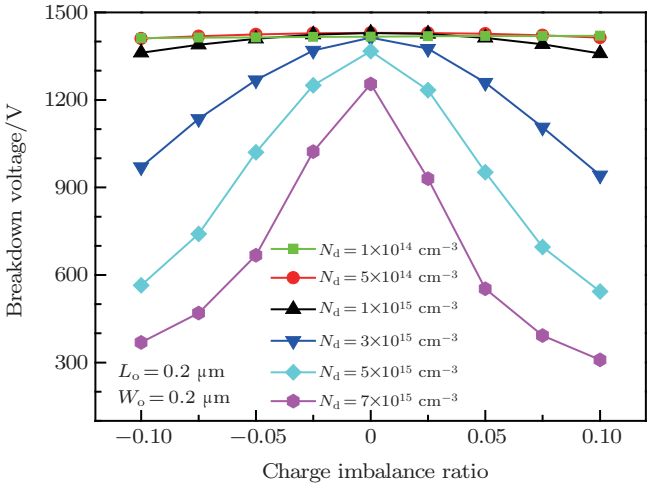


Fig. 6. (color online) Influences of charge imbalance ratio on BV.

Figure 7 shows the influences of W_o and L_o on $V_{ce(on)}$ and BV for the BO-SJ IGBT device. It can be seen that for different values of L_o, $V_{ce(on)}$ decreases as W_o decreases. The bigger the L_o, the smaller the $V_{ce(on)}$ which can be obtained. For BV, however, W_o has almost no influence on it even with different values of L_o. Figure 8 shows the influences of W_o and L_o on the tradeoff between $V_{ce(on)}$ and E_{off} for the proposed structure. It can be seen that an improved tradeoff performance can be obtained with a smaller W_o and a bigger L_o.

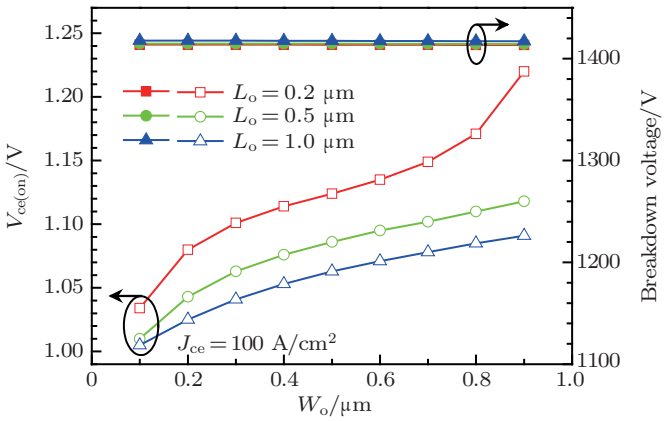


Fig. 7. (color online) Influences of W_o and L_o on $V_{ce(on)}$ and BV.

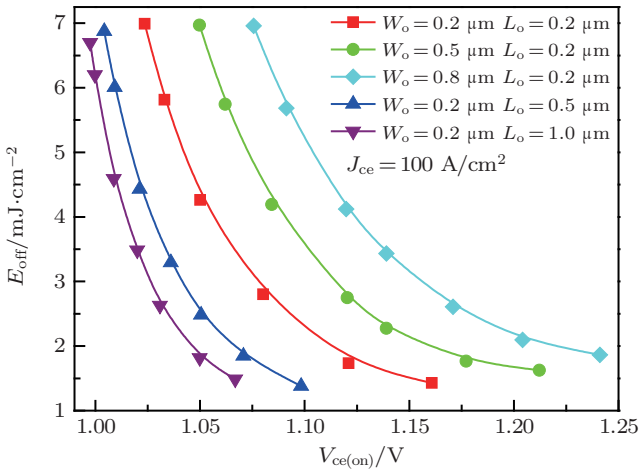


Fig. 8. (color online) Influences of W_o and L_o on the tradeoff.

The distributions of minority carriers along AA' and BB' lines for the proposed structure with different values of W_o and L_o are shown in Figs. 9(a) and 9(b). The majority carriers along AA' and BB' lines also have similar distributions. It can be seen that with a smaller W_o and a bigger L_o the concentration of the carriers in the drift region increases significantly, especially in the emitter side of the drift region. This indicates that a further reduced $V_{ce(on)}$ and an improved tradeoff performance are derived from further optimized carrier distribution in the SJ drift region.

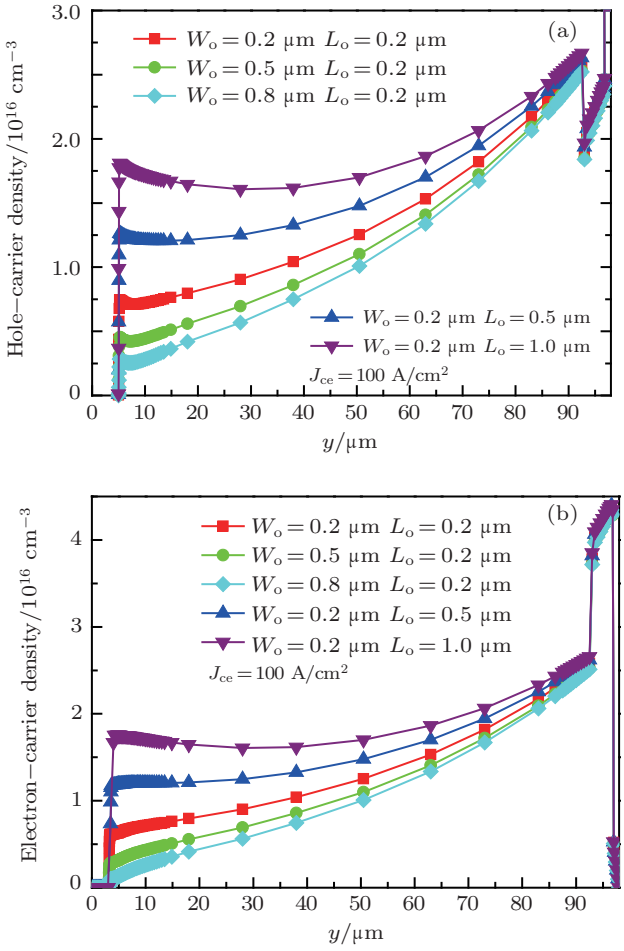


Fig. 9. (color online) Distributions of minority carriers along (a) AA' line and (b) BB' line for the proposed structure.

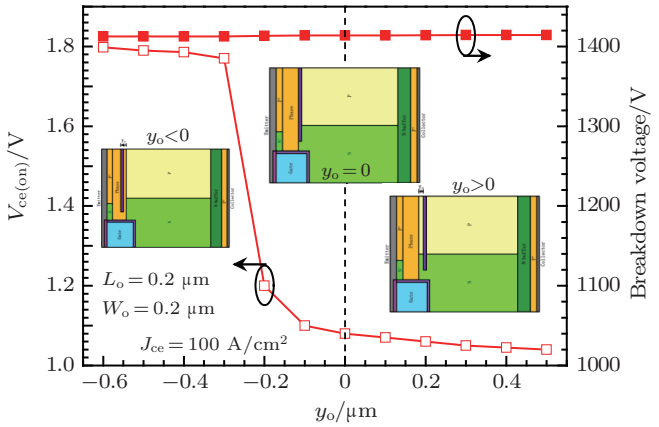


Fig. 10. (color online) Influences of the BO layer vertical position y_o on $V_{ce(on)}$ and BV.

Figure 10 shows the influences of the BO layer vertical position y_o on $V_{ce(on)}$ and BV for the BO-SJ IGBT device. It can be seen that when the BO layer moves from the P-pillar ($y_o > 0$) to the P_{base} ($y_o < 0$), the $V_{ce(on)}$ increases slowly as y_o decreases apart from a sudden increase at $y = -0.3$ μm. Further analysis indicates that a hole carrier path is formed underneath the BO layer during the on-state with $y \leq -0.3$ μm due to the connection of the P-pillar to P_{base}. The formation of the

hole carrier path significantly reduces the conduction modulation in the emitter side of the SJ drift region. It can also be seen that the smaller position change of the BO layer has almost no influence on *BV* due to the full depletion of the SJ region. This indicates that a wide vertical position tolerance is available for the BO-SJ IGBT structure as long as $y \geq -0.2$ μm.

4. Conclusion

A novel high performance TFS SJ IGBT with BO layer is proposed in this paper. Detailed numerical analysis is performed to understand the operating mechanism. The simulated results show that compared with the Conv-SJ, the proposed BO-SJ IGBT structure has an enhanced conduction modulation in the emitter side of the SJ drift region and an optimized carrier distribution in the drift region. As a result, compared with the Conv-SJ, the proposed structure has a drastically reduced $V_{ce(on)}$ and an improved $V_{ce(on)} - E_{off}$ tradeoff, with no *BV* degraded.

References

[1] Mori M, Saitou R and Yatsuo T 1993 *Proceedings of the IEEE 5th International Symposium on Power Semiconductor Devices & IC's*, May 18–20, 1993, Monterey, USA, p. 287

[2] Onozawa Y, Otsuki M, Iwamuro N, Miyashita S, Miyasaka T, Seki Y and Matsumoto T 2007 *IEEE Trans. Industry Applications* **43** 513

[3] Ranstad P and Nee H P 2011 *IEEE Trans. Power Electronics* **26** 260

[4] Ogura T, Ninomiya H, Sugiyama K and Inoue T 2004 *IEEE Trans. Electron Dev.* **51** 636

[5] Nakamura H, Nakamura K, Kusunoki S, Takahashi H, Tomomatsu Y and Harada M 2001 *Proceedings of the IEEE 13th International Symposium on Power Semiconductor Devices & IC's*, June 4–7, 2001, Osaka, Japan, p. 299

[6] Zhang J, Li Z, Zhang B and Li Z 2012 *Electron. Lett.* **48** 525

[7] Zhang J P, Li Z H, Zhang B and Li Z J 2012 *Chin. Phys. B* **21** 068504

[8] Takei M, Fujikake S, Nakazawa H, Naito T, Kawashima T, Shimoyama K and Kuribayashi H 2010 *Proceedings of the IEEE 22nd International Symposium on Power Semiconductor Devices & IC's*, June 6–10, 2010, Hiroshima, Japan, p. 383

[9] Watanabe S, Mori M, Arai T, Ishibashi K and Toyoda Y 2011 *Proceedings of the IEEE 23rd International Symposium on Power Semiconductor Devices & IC's*, May 23–26, 2011, San Diego, USA, p. 48

[10] Sumitomo M, Asai J, Sakane H, Arakawa K, Higuchi Y and Matsui M 2012 *Proceedings of the IEEE 24th International Symposium on Power Semiconductor Devices & IC's*, June 3–7, 2012, Bruges, Belgium, p. 17

[11] Chen X 1993 US Patent 5216275

[12] Chen X and Sin J K O 2001 *IEEE Trans. Electron Dev.* **48** 344

[13] Chen Y, Liang Y C, Samudra G S, Yang X, Buddharaju K D and Feng H 2008 *IEEE Trans. Electron Dev.* **55** 211

[14] Bartolf H, Mihaila A, Nistor I, Jurisch M, Leibold B and Zimm M 2013 *IEEE Trans. Semiconductor Manufacturing* **26** 529

[15] Li Z, Ren M, Zhang B, Ma J, Hu T, Zhang S, Wang F and Chen J 2010 *J. Semicond.* **31** 084002-1

[16] Oh K H, Lee J, Lee K H, Kim Y C and Yun C 2006 *IEEE Trans. Electron Dev.* **53** 884

[17] Yuan S C and Liu Y M 2008 *IEEE Electron Dev. Lett.* **29** 931

[18] Antoniou M, Udrea F and Bauer F 2010 *IEEE Trans. Electron Dev.* **57** 594

[19] Bauer F, Nistor I, Mihaila A, Antoniou M and Udrea F 2012 *IEEE Electron Dev. Lett.* **33** 1288

[20] Bruel M, Aspar B, Charlet B, Maleville C, Poumeyrol T and Soubie A 1995 *Proceedings of the IEEE International SOI Conference*, October 3–5, 1995, Tucson, USA, p. 178

[21] Tong Q, Cha G, Gafiteanu R and Gosele U 1994 *Journal of Microelectromechanical Systems* **3** 29